



Published in final edited form as:

*J Bone Miner Res.* 2020 April ; 35(4): 681–690. doi:10.1002/jbmr.3939.

## Heterogeneous spatial and strength adaptation of the proximal femur to physical activity: a within-subject controlled cross-sectional study

Stuart J. Warden<sup>1,2,3</sup>, Julio Carballido-Gamio<sup>4</sup>, Alyssa M. Weatherholt<sup>5</sup>, Joyce H. Keyak<sup>6</sup>, Chenxi Yan<sup>7</sup>, Mariana E. Kersh<sup>7</sup>, Thomas F. Lang<sup>8</sup>, Robyn K. Fuchs<sup>1,2</sup>

<sup>1</sup>Department of Physical Therapy, School of Health and Human Sciences, Indiana University, Indianapolis, IN;

<sup>2</sup>Indiana Center for Musculoskeletal Health, Indiana University, Indianapolis, IN;

<sup>3</sup>La Trobe Sport and Exercise Medicine Research Centre, La Trobe University, Bundoora, Victoria, Australia;

<sup>4</sup>Department of Radiology, School of Medicine, University of Colorado Anschutz Medical Campus, Aurora, CO;

<sup>5</sup>Department of Kinesiology and Sport, Pott College of Science, Engineering, and Education, University of Southern Indiana, Evansville, IN;

<sup>6</sup>Departments of Radiological Sciences, Mechanical and Aerospace Engineering, and Biomedical Engineering, University of California Irvine, Irvine CA;

<sup>7</sup>Department of Mechanical Science and Engineering, College of Engineering, University of Illinois at Urbana-Champaign, Urbana-Champaign, IL;

<sup>8</sup>Department of Radiology and Biomedical Imaging, School of Medicine, University of California San Francisco, San Francisco, CA

### Abstract

Physical activity (PA) enhances proximal femur bone mass, as assessed using projectional imaging techniques. However, these techniques average data over large volumes obscuring spatially heterogeneous adaptations. The current study used quantitative computed tomography, statistical parameter mapping, and subject-specific finite element (FE) modeling to explore spatial adaptation of the proximal femur to PA. In particular, we were interested in adaptation occurring at the superior femoral neck and improving strength under loading from a fall onto the greater trochanter. High/long jump athletes (n=16) and baseball pitchers (n=16) were utilized as within-

---

**Address correspondence to:** Stuart J. Warden, PT, PhD, Department of Physical Therapy, School of Health and Human Sciences, Indiana University, 1140 W. Michigan St., CF-120, Indianapolis, IN 46202. Telephone: 317-278-8401. stwarden@iu.edu. Authors' roles: Study design: SJW, JCG, AMW, MEK, and RKF. Data analysis: SJW, JCG, AMW, JHK, CY, MEK, TFL, and RKF. Data interpretation: SJW, JCG, AMW, JHK, CY, MEK, TFL, and RKF. Drafting manuscript: SJW and RKF. Revising manuscript content and approving final version of manuscript: SJW, JCG, AMW, JHK, CY, MEK, TFL, and RKF. SJW and RKF take responsibility for the integrity of the data analysis.

### DISCLOSURES

All authors state that they have no conflicts of interest.

subject controlled models as they preferentially load their takeoff leg and leg contralateral to their throwing arm, respectively. Controls (n=15) were included, but did not show any dominant-to-nondominant (D-to-ND) leg differences. Jumping athletes showed some D-to-ND leg differences, but less than pitchers. Pitchers had 5.8% (95% CI, 3.9–7.6%) D-to-ND leg differences in total hip volumetric bone mineral density (vBMD), with increased vBMD in the cortical compartment of the femoral neck, and trochanteric cortical and trabecular compartments. Voxel-based morphometry analyses and cortical bone mapping showed pitchers had D-to-ND leg differences within the regions of the primary compressive trabeculae, inferior femoral neck, and greater trochanter, but not the superior femoral neck. FE modeling revealed pitchers had 4.1% (95% CI, 1.4–6.7%) D-to-ND leg differences in ultimate strength under single-leg stance loading, but no differences in ultimate strength to a fall onto the greater trochanter. These data indicate the asymmetrical loading associated with baseball induces proximal femur adaptation in regions associated with weight bearing and muscle contractile forces, and increases strength under single-leg stance loading. However, there were no benefits evident at the superior femoral neck and no measurable improvement in ultimate strength to common injurious loading during aging (i.e. fall onto the greater trochanter) raising questions as to how to better target these variables with PA.

### Keywords

bone; exercise; falls; femoral neck fracture; osteoporosis

## INTRODUCTION

The proximal femur is a frequent target for physical activity-induced bone adaptation as osteoporotic fractures at this site are a significant cause of morbidity and mortality. A large body of evidence has demonstrated benefits of physical activity on proximal femur bone health;<sup>(1–3)</sup> however, questions remain as to whether the benefits translate into an enhanced ability to resist fracture related loading.<sup>(4)</sup>

Any region of the proximal femur can fracture under the right loading conditions; however, femoral neck fractures are most concerning as they have the greatest risk for complication. Femoral neck fractures in the elderly typically occur due to a fall in a direction broadly classified as “sideways” and with impact on the greater trochanter.<sup>(5)</sup> The proximal femur is 3 times more likely to fracture during a sideways fall compared to a forward or backward fall, and over 30-times more likely to fracture if the fall impacts the greater trochanter.<sup>(6)</sup>

The heightened fracture risk during a fall onto the greater trochanter partly results from the heterogeneous structure of the femoral neck, whose design reflects adaptation to stereotypical locomotor-related forces.<sup>(7)</sup> The femoral neck experiences maximum compressive stresses inferiorly and smaller tensile stresses superiorly during gait.<sup>(8–10)</sup> To accommodate this habitual asymmetrical loading, the femoral neck possesses a much thicker inferior than superior cortex, and an associated trabecular network positioned to resist and transmit weight-bearing directed loads.<sup>(11)</sup>

In contrast to during gait, the stress pattern within the femoral neck is reversed during a fall onto the greater trochanter. Greatest compressive stresses now occur about the thin superior

cortex, which includes the upper quadrant of the femoral neck extending from the head-neck junction to the trochanteric fossa, while the thick inferior cortex is exposed to lower tensile stresses.<sup>(9–12)</sup> The net result is exposure of the superior cortex to unaccustomed, potentially injurious stresses, as seen during *in vitro* simulated falls onto the greater trochanter with fracture initiation occurring within the superior region.<sup>(13, 14)</sup>

The heightened susceptibility of the superior femoral neck to fracture during a fall onto the greater trochanter makes this a region of interest with regards to fracture prevention strategies. It also raises the question as to whether physical activity-induced bone adaptation occurs at this location. Initial studies using three-dimensional (3D) imaging techniques have explored adaptation of the superior femoral neck to physical activity, but the data remains inconclusive.<sup>(15–18)</sup> Some studies suggested physical activity may positively influence the superior femoral neck,<sup>(15, 16)</sup> whereas others reported no effect.<sup>(17, 18)</sup>

The aim of the current study was to explore spatial adaptation of the proximal femur to chronic physical activity, and to evaluate whether adaptation occurred at the superior femoral neck and influenced strength under loading from a fall onto the greater trochanter. Jumping (long and high jump) athletes and baseball pitchers were utilized as within-subject controlled models as they preferentially load their takeoff leg and the leg contralateral to their throwing arm, respectively. Both athlete groups exhibit side-to-side differences (i.e. bilateral asymmetry) in proximal femoral bone health, as assessed using dual-energy x-ray absorptiometry.<sup>(19)</sup> Control subjects were included to account for crossed asymmetry whereby the lower extremity opposite the dominant arm may possess enhanced proximal femur bone properties.<sup>(20)</sup> Statistical parameter mapping (SPM) was used to assess localized dominant-to-nondominant (D-to-ND) leg differences in the spatial distribution of bone properties, and subject-specific finite element (FE) modeling was used to explore D-to-ND leg differences in proximal femur strength under loads during single-leg stance and a fall onto the greater trochanter.

## MATERIALS AND METHODS

### Study design and participants

A within-subject controlled cross-sectional study design was implemented to compare the bilateral proximal femurs in male jumping athletes ('jumpers'), baseball pitchers ('pitchers'), and controls. Leg dominance in each group was defined as follows: jumpers—the leg the participant jumps/takes off from during long and/or high jump; pitchers—the leg opposite the pitching arm, and; controls—the leg opposite the dominant arm.

Subjects were eligible to participate if aged 18–30 years and in good general health. Jumpers were included if currently competing or practicing in long and/or high jump within the National Collegiate Athletic Association (Division I, II or III level). Pitchers were included if currently competing as a pitcher in professional Minor League Baseball (Triple-A level). Controls were included if they did not have a past history of participating more than twice per month for >6 months in an activity that may expose the lower extremities to asymmetrical loading (e.g. soccer, fencing, ten-pin bowling, baseball, softball, etc.).

Exclusion criteria for all groups were: 1) known metabolic bone disease; 2) history of a femoral fracture or stress fracture; 3) implanted metal within the femur, and; 4) exposure to lower extremity immobilization for more than 2 weeks within the past 2 years. The study was approved by both the Institutional Review Board and Machine Produced Radiation Safety Committee of Indiana University (study ID#1503934363), and all participants provided written informed consent.

### **Dual-energy x-ray absorptiometry (DXA)**

A whole-body DXA scan (Discovery-W machine with Apex v2.3 software; Hologic, Inc., Waltham, MA, USA) was performed using the manufacturer's standard scan and positioning protocol to acquire whole-body aBMD ( $\text{g}/\text{cm}^2$ ), and whole-body lean (kg) and percent fat (%) mass. Bilateral femurs were imaged, with the obtained data being reported elsewhere. (19)

### **Quantitative computed tomography**

Bilateral proximal femurs were imaged during a single pelvic scan on a multislice CT scanner (Biograph128 mCT; Siemens Healthcare, Knoxville, TN) operating at 120 kVp, 320 mAs, 128 $\times$ 0.6 collimation, and pitch 0.8. A scan region spanning from 1 cm superior to the acetabulum to 5 cm distal to the lesser trochanter was prescribed from a scout scan. The scan volume included a calibration phantom containing calcium hydroxyapatite standards embedded in water-equivalent resin (QCT-Bone Mineral Phantom; Image Analysis, Inc., Columbia, KY). Images were axially reconstructed at 1.0 mm slice thickness  $\times$  1.0 mm slice thickness using a B60s convolution kernel, 512 $\times$ 512 matrix and reconstruction diameter of 50 cm (reconstructed voxel size = 0.976  $\times$  0.976  $\times$  1.0 mm<sup>3</sup>).

### **Volumetric bone mineral density**

Volumetric bone mineral density (vBMD) was computed using semi-automated software.<sup>(21)</sup> In brief, QCT images were reformatted along the femoral neck axis, and a region growing algorithm was applied to extract the proximal femur from the surrounding soft tissue. Three measurement regions were automatically defined encompassing the total proximal femur, femoral neck, and lesser and greater trochanters. Integral (i.e., total), cortical, and trabecular vBMD were computed within each region, with the linear relationship between Hounsfield Units and densities of the calcium hydroxyapatite standards within the co-scanned phantom used to determine voxel density ( $\text{mg}/\text{cm}^3$ ). We observed root mean square coefficients of variation (RMS-CVs) for vBMD outcomes of <1.7% for duplicate scans in 22 individuals. (22, 23)

### **Voxel- and vertex-based analyses**

SPM was used to assess for localized D-to-ND leg differences in the spatial distribution of bone properties. In particular, voxel-based morphometry was used for vBMD,<sup>(24)</sup> and cortical bone mapping for cortical vBMD (Ct.vBMD), cortical thickness (Ct.Th),<sup>(22, 25)</sup> and vBMD in a layer adjacent to the endosteal surface (EndoTb.vBMD).<sup>(26)</sup> Proximal femur images from the nondominant leg were mirrored to those of the dominant leg, and the segmented bones spatially normalized to a minimum deformation template representing the

average size and shape of all proximal femora in the study. The spatial normalizations reduced the anatomical variability among the femora, effectively establishing anatomical correspondences locally. The computed transformations were then applied to the vBMD maps and to the surface-based maps of Ct.vBMD, Ct.Th and EndoTb.vBMD, enabling voxel-wise and vertex-wise D-to-ND leg comparisons. Registrations to build the minimum deformation template and for the spatial normalizations included affine and nonlinear transformations. We measured RMS-CVs of <4% and small absolute precision errors for surface-based mean Ct.vBMD and Ct.Th for duplicate scans in 22 individuals.<sup>(22)</sup>

### Finite element modeling

Proximal femur strengths under load conditions of single-leg stance and a fall onto the posterolateral aspect of the greater trochanter were estimated using FE models, as previously described.<sup>(27–32)</sup> Loading in a posterolateral (as opposed to lateral or posterior) direction was modeled as this direction provides information about incident hip fracture in men beyond BMD.<sup>(32)</sup> For both conditions, heterogeneous linear elastic and nonlinear post-yield material properties computed from CT-measured vBMD were used to describe the stress-strain relationship for each 3-mm cube of bone that was represented by a linear hexahedral finite element.<sup>(28, 32)</sup> Ultimate strengths under stance and fall loading were obtained by incrementally applying displacement to the femoral head while allowing motion in the direction perpendicular to the displacement, and the distal end was fully constrained. For stance loading, displacement was applied within the coronal plane at 20 degrees to the shaft axis. For fall loading, displacement was applied at 35 degrees to the coronal plane and 80 degrees to the shaft axis (angles measured within planes containing the displacement vector). The surface of the greater trochanter opposite the loaded surface of the femoral head was constrained in the direction of displacement while allowing motion perpendicular to the displacement. As displacement on the femoral head was incrementally applied, element stress and strain were computed using the individual element's stress-strain relationship in conjunction with the von Mises yield criterion. The reaction force on the femoral head was computed at each increment, which resulted in a computed force versus displacement curve for the proximal femur. Thus, according to established engineering principles, the FE-computed proximal femur strength was the maximum FE-computed force on the femoral head. To more deeply evaluate the fracture process under fall loading, the yield strength under fall loading was obtained by applying force to the femoral head and identifying the force at which 15 contiguous nonsurface elements had yielded according to the von Mises yield criterion.<sup>(30, 31)</sup> We previously identified RMS-CVs of 3.5–3.6% for stance and fall loading bone strength for duplicate scans in 22 individuals.<sup>(22)</sup>

### Statistical analyses

Two-tailed analyses with  $\alpha = 0.05$  were performed with IBM SPSS Statistics (v25; SPSS Inc., Chicago, IL). Demographic and anthropometric characteristics, and femur properties in the ND leg were compared between groups using a one-way ANOVA followed by a Fisher's least square difference post-hoc test. Whole-body lean mass was used as a covariate in the comparisons of ND leg femur properties.

D-to-ND leg differences for vBMD and estimated strength were assessed by calculating mean percent differences ( $[D-ND]/ND \times 100\%$ ) and their 95% confidence intervals (CI). 95% CIs not crossing zero were statistically significant, as determined by single sample t-tests (population mean = 0%). D-to-ND leg percent difference values were compared between groups using a one-way ANOVA followed by a Fisher's least square difference post-hoc test.

Voxel-wise and vertex-wise D-to-ND leg differences were determined using linear mixed-effects models with a random intercept, allowing for age, height, weight, and shape as follows:

$$\text{Bone property} = b_0 + b_1 * \text{Leg} + b_2 * \text{Age} + b_3 * \text{Height} + b_4 * \text{Weight} + b_5 * \text{PC1Shape} + b_6 * \text{PC2Shape} + b_7 * \text{PC3Shape} + b_8 * \text{PC4Shape} + b_9 * \text{PC5Shape} + (1|\text{Subject}) + \text{error}$$

where: bone property = vBMD, Ct.vBMD, Ct.Th or EndoTb.vBMD; leg = 0 for nondominant and 1 for dominant; age, height and weight were the same for both legs as comparisons were within-subject; and PC1Shape-PC5Shape were computed for each leg and represented the first 5 modes of shape.<sup>(33, 34)</sup> The local comparisons performed with the above equation yielded a Student's t-test map (t-map) for  $b_1$  and its corresponding P-value map, which was corrected for multiple comparisons using false discovery rate correction ( $q=0.05$ ).<sup>(35)</sup> Significant voxels after correction indicated significant differences in vBMD, while significant vertices after FDR correction indicated significant D-to-ND leg differences in Ct.vBMD, Ct.Th or EndoTb.vBMD.

## RESULTS

### Participant characteristics

There were 15, 16, and 16 controls, jumpers, and pitchers, respectively (Table 1). Pitchers were older, taller, heavier, and had greater BMI and whole-body fat mass than both jumpers and controls (all  $p < 0.05$ ). Pitchers started competing younger and had been competing for longer than jumpers (all  $p < 0.05$ ). Jumpers were heavier with greater BMI than controls ( $p < 0.05$ ), and both pitchers and jumpers had greater whole-body aBMD and lean mass than controls (all  $p < 0.05$ ). These between group differences in whole-body anthropometric measures are not considered to influence within-subject proximal femur asymmetry as they are normalized when calculating D-to-ND leg differences.

Jumpers had greater integral vBMD within the ND leg at both the total proximal femur and trochanter, and greater trabecular vBMD at both the total proximal femur and femoral neck than controls (all  $p < 0.02$ ; Supplementary Table 1). Jumpers had 29–30% greater ultimate strength during single-leg stance and 43–53% greater yield strength during a fall onto the posterolateral greater trochanter in their ND leg than in both controls and pitchers (all  $p < 0.001$ ; Supplementary Table 2). There were no group differences in ultimate strength of the proximal femur in the ND leg during a fall onto the posterolateral greater trochanter (all  $p = 0.18$  to 0.88, Supplementary Table 2). There were no differences in the ND leg between controls and pitchers for any proximal femur vBMD or estimated strength measure (all  $p = 0.16$  to 0.91).



## vBMD

There were no D-to-ND leg differences in vBMD in controls (all  $p=0.06$  to  $0.67$ ; Fig. 1 and Supplementary Table 1). Jumpers and pitchers had D-to-ND leg differences in integral vBMD at both the total proximal femur and femoral neck (all  $p < 0.03$ ) (Fig. 1A,D). The 5.8% (95% CI, 3.9 to 7.6%) D-to-ND leg difference for integral vBMD at the total proximal femur in pitchers was greater than observed in both jumpers and controls (all  $p < 0.002$ ) (Fig. 1A). Pitchers also had D-to-ND leg differences for integral vBMD at the trochanter ( $p < 0.001$ ), which were greater than that in both jumpers and controls (all  $p < 0.002$ ) (Fig. 1G).

The D-to-ND leg differences in integral vBMD at the total proximal femur and femoral neck in jumpers resulted from D-to-ND leg differences in cortical vBMD (all  $p < 0.01$ ; Fig. 1B,E), as opposed to differences in trabecular vBMD ( $p = 0.39$  to  $0.62$ ; Fig. 1C,F). In contrast, D-to-ND leg differences in integral vBMD at the total proximal femur in pitchers resulted from D-to-ND leg differences in both cortical (all  $p < 0.001$ ; Fig. 1B) and trabecular ( $p = 0.008$ ; Fig. 1C) vBMD, with the differences for trabecular vBMD being greater than in both jumpers and controls (all  $p < 0.01$ , Fig. 1C). The D-to-ND leg differences for integral vBMD at the trochanters in pitchers resulted from D-to-ND leg differences in both cortical ( $p < 0.05$ ; Fig. 1H) and trabecular ( $p = 0.008$ ; Fig. 1I) vBMD, with the differences for trabecular vBMD being greater than in both jumpers and controls (all  $p < 0.02$ , Fig. 1I).

### Voxel-wise distribution of vBMD

There were no voxel-wise D-to-ND leg differences in vBMD in controls. Jumpers exhibited D-to-ND leg differences (positive t-values) for vBMD in regions along a line connecting the superomedial femoral head, inferior femoral neck and medial intertrochanteric region (Fig 2A). Jumpers also had D-to-ND leg differences for vBMD within the greater trochanter. A couple of small islands of voxels in the superior femoral neck of jumpers exhibited D-to-ND leg differences in vBMD.

The D-to-ND distribution of elevated vBMD in pitchers exhibited a similar, but more expansive pattern to that observed in jumpers (Fig. 2B). The region of greater vBMD (positive t-values) connecting the superomedial femoral head, inferior femoral neck and medial intertrochanteric region was more continuous and included more voxels in pitchers compared to jumpers. Similarly, the D-to-ND leg difference in the region of the greater trochanter had more voxels with elevated vBMD when compared to jumpers. Greatest t-values for D-to-ND leg differences in pitchers were observed in the posterior aspect of the greater trochanter and posterolateral aspect of the proximal diaphysis. There were two regions within the posterior femoral head of lesser vBMD (negative t-values) in dominant compared to nondominant legs in pitchers. No voxels in the superior femoral neck of pitchers exhibited D-to-ND leg differences in vBMD.

### Vertex-wise distribution of cortical vBMD, Ct.Th and EndoTb.vBMD

There were no significant vertex-wise D-to-ND leg differences in controls. Jumpers had areas of D-to-ND leg differences in Ct.vBMD and Ct.Th at the greater trochanter and inferior femoral neck, respectively (Fig. 3A,B). There were few and small areas of D-to-ND

leg differences in EndoTb.vBMD in jumpers (Fig. 3C). There were negligible areas of increased D-to-ND leg differences in Ct.vBMD, Ct.Th or EndoTb.vBMD at the superior femoral neck in jumpers.

Pitchers had large areas of D-to-ND leg differences in cortical vBMD at the greater trochanter (Fig. 4A) and Ch.Th at the inferior femoral neck (Fig. 4B). In addition, pitchers had D-to-ND leg differences in EndoTb.vBMD at the greater trochanter and a patch at the inferior femoral neck (Fig. 4C). There were no areas of D-to-ND leg differences in Ct.vBMD, Ct.Th or EndoTb.vBMD at the superior femoral neck in pitchers.

### Estimated strength of the proximal femur

For both single-leg stance loading and loading associated with a fall onto the greater trochanter, fracture initiation was located within the trabecular bone and was not in contact with elements whose nodes were constrained, similar to previously published findings.<sup>(30, 36)</sup> Fracture did not involve the boundary conditions because the surface elements to which the boundary conditions were applied were stiffened and covered a large enough region to prevent stress concentrations. Yield and plastic deformation then progressed to a subcapital or neck fracture for the stance loading condition and an intertrochanteric or neck fracture for the fall loading condition.

There were no D-to-ND leg differences in estimated strength measures in controls (all  $p > 0.05$ ) or jumpers (all  $p > 0.05$ ) (Fig. 5 and Supplementary Table 2). Pitchers had 4.1% (95% CI, 1.4 to 6.7%) D-to-ND leg differences in ultimate strength under single-leg stance loading ( $p < 0.01$ ; Fig. 5A) and 12.8% (95% CI, 2.3 to 23.3%) D-to-ND leg differences in yield strength under loading from a fall onto the greater trochanter ( $p < 0.05$ ; Fig. 5B), with the differences being greater than in controls (all  $p < 0.05$ ). No group had D-to-ND leg differences in ultimate strength under loading from a fall onto the greater trochanter (all  $p = 0.21$  to  $0.77$ ) (Fig. 5C).

## DISCUSSION

The current data reveal spatially heterogeneous adaptation of the proximal femur to mechanical loading associated with weight bearing physical activity. Using baseball pitchers and jumping athletes as within-subject controlled models of asymmetrical lower extremity loading, proximal femur vBMD was greater in the leg opposite the throwing arm in baseball pitchers and, to a lesser extent, the take-off leg in jumping athletes. No side-to-side differences were observed in control subjects. These data are consistent with DXA-derived data from the same individuals,<sup>(19)</sup> and observations of elevated unilateral loading during baseball pitching and jumping.<sup>(37–42)</sup> However, assessment of subvolumes of tissue revealed the adaptation was principally localized to a line connecting the superomedial femoral head, inferior femoral neck, and medial intertrochanteric regions. Adaptation was also evident at the greater trochanter. In contrast, there was no to minimal adaptation at the superior region of the femoral neck.

The adapted sites within the femoral neck correspond with the primary compressive trabecular network and inferior cortex, regions thought to support and transmit weight-



bearing directed loads.<sup>(8–10)</sup> Accordingly, the adaptation observed in pitchers resulted in increased predicted strength of the proximal femur to loading in the direction of single-leg stance. In contrast, there was a lack of any appreciable tissue adaptation in the superior femoral neck region. This region is clinically relevant as it is exposed to greatest stress/strain during impact from a fall onto the greater trochanter;<sup>(9–12)</sup> femoral neck fractures appear to initiate in the region during a sideways fall;<sup>(13, 14)</sup> the region experiences greater bone loss during aging compared to the more preserved inferior femoral neck,<sup>(24, 43)</sup> and; deficits in the region are associated with incident femoral neck fracture.<sup>(26, 34, 44, 45)</sup>

The lack of adaptation at the superior femoral neck was coupled with an absence of side-to-side differences in proximal femur ultimate strength under loading from a fall onto the greater trochanter, the type of loading most associated with femoral neck fractures during aging. There were D-to-ND leg differences in pitchers in yield strength under fall loading, indicating an enhanced ability to resist plastic deformation and damage initiation. On inspection, yield tended to occur within the greater trochanter with the higher yield in the D leg in pitchers likely reflecting the adaptation observed in the region. In contrast, there was a lack of a D-to-ND leg difference in ultimate strength suggesting no enhanced ability to withstand force before the proximal femur broke in the intertrochanteric or neck region.

A large body of evidence has revealed benefits of weight-bearing physical activity on proximal femur bone health;<sup>(3)</sup> however, studies have traditionally relied on projectional 2D DXA-derived outcomes which have known limitations in assessing site-specific adaptation of bone to physical activity related loading.<sup>(46, 47)</sup> The current data indicate that an increase in bone mass/density does not necessary confer an increase in bone strength as the location mineral is deposited relative to mechanical axes is also an important factor. Unlike simple bone density measures, FE analyses can determine if and to what extent a change in density at a particular location influences whole bone strength.

The FE model we used to predict proximal femur ultimate strength under posterolateral fall loading has been shown to predict cadaveric femora strength as well as prospectively distinguish males who went on to suffer a hip fracture even after considering the contribution of aBMD.<sup>(32)</sup> After accounting for the age and sex of the male subjects in the present study, the proximal femur ultimate strength estimates obtained are consistent with those previously obtained for 397 male and female subjects aged 27 to 90 years.<sup>(48)</sup>

It is possible that ultimate strength was improved under fall-related loading in a direction different from that modeled or that the adaptation observed within the inferior neck conferred benefits that were not detected because of insufficient statistical power. When bending the femoral neck, material on both sides of the neutral axis contribute to resisting the applied force. Adaptation of the inferior neck would present a greater inferior area to absorb bending forces and create an inferior shift of the neutral axis. The inferior shift would increase the area of bone above the axis over which compressive forces act during a fall onto the greater trochanter and, thereby, reduce the stress/strain per given external load to provide indirect protection to the superior neck. *Post hoc* analyses using the acquired data indicated that we could detect D-to-ND leg differences of 5.5% for ultimate strength under loading from a fall onto the greater trochanter, which may not have been sufficient to identify any

benefits conferred from the changes observed at the inferior neck and shift in the neutral axis. We did observe improved bone properties at the greater trochanter with physical loading, likely due to muscle contractile forces, which may protect against greater trochanteric fractures. Deficits in the greater trochanter region have been associated with risk of greater trochanteric fracture.<sup>(26, 34, 45)</sup>

Our data are not the first to explore adaptation in sub-volumes of the proximal femur to physical activity. Previous cross-sectional studies by Sievänen and colleagues<sup>(15, 18, 49)</sup> reported individuals competing in impact sports introducing multidirectional loading did not have elevated cortical thickness within the superior cortex of the femoral neck, but FE models did show reduced von Mises stresses at this location and increased overall fracture load during a simulated fall. However, the data were collected using a between-subjects study design which does not account for selection bias and their FE models were based on magnetic resonance imaging data which included patient-specific bone geometry, but did not take into account bone material properties.

Two studies<sup>(16, 17)</sup> longitudinally mapped proximal femur adaptation to physical activity applying similar approaches to those used in the current study. Allison and colleagues<sup>(16)</sup> performed a 12-month randomized, within-subject controlled study of daily, high-impact, unilateral, multidirectional hopping in elderly males. Cortical bone mapping identified increases in cortical mass surface density and endocortical trabecular density in the inferoanterior femoral neck and greater trochanter, with some potential adaptation reported in the superior femoral neck. However, changes in regional bone properties over time in the exercised leg were not statistically compared to those in the contralateral control leg. As a consequence, it remains unclear whether the exercise intervention significantly induced changes beyond normal maturation over time or improved resistance to fall loading.

Lang et al.<sup>(17)</sup> used VBM and CT-based FE models to explore proximal femur adaptation over 16 weeks to non-weight bearing hip abduction/adduction exercises or closed-kinetic chain (i.e. weight bearing) squats and deadlifts, or a combination of both. The non-weight bearing exercises induced adaptation at muscle insertion sites (i.e. greater trochanter), but did not impact FE-computed fracture load. In contrast, the weight bearing exercises induced adaptation primarily in the inferior femoral neck and improved fracture load in single-leg stance. However, there was no adaptation at the superior femoral neck or change in fracture load from a posterolateral fall onto the greater trochanter, consistent with the current study. Though, it is possible 16 weeks was not long enough to induce measurable superior femoral neck adaptation in the study by Lang et al.<sup>(17)</sup>

The inability of conventional weight bearing activities to induce adaptation at the superior femoral neck and improve bone strength under posterolateral fall loading raises the question as to how to load, adapt and strengthen the region. We know the superior femoral neck is exposed to loading as it is a site for high-risk tensile stress fractures. We also know that the region is responsive to intervention, with denosumab increasing superior femoral neck cortical bone mass and thickness.<sup>(50)</sup> One thought is that activities need to load the proximal femur in less habitual directions. Each of the previous studies mapping proximal femur adaptation to physical activity incorporated some component of multidirectional loading,

including odd impacts, hopping in a variety of directions, and non-weight bearing hip abduction/adduction exercises.<sup>(15–18, 49)</sup> However, the general lack of benefit on the superior femoral neck suggests other loading modalities need to be considered.

It is possible that hip position during loading is important for targeting the superior femoral neck. We recently used a subject-specific musculoskeletal model of the lower extremity and CT-based FE model of the proximal femur to show weight bearing loading with the hip in flexion (e.g. during stair ascent) engendered greatest strain within the superior femoral neck in postmenopausal women.<sup>(8)</sup> An alternative research group suggested stair descent loaded the superior femoral neck more so than stair ascent, but the study applied forces to a generic elliptical femoral neck cross-sectional model as opposed to a subject-specific FE proximal femur model raising concerns regarding model accuracy.<sup>(51)</sup> Martelli and colleagues<sup>(52)</sup> produced data suggesting maximal hip extension and knee flexion exercises maximally loaded the thinnest region of the superior femoral neck; however, data were limited to the study of a single individual and the application of musculoskeletal loads calculated from a young volunteer to an FE model of the proximal femur from an older individual. There is a definite need for further studies to model proximal femur and particularly femoral neck loading to better define activities that may target and adapt the superior femoral neck.

In comparison to baseball pitchers, there were limited D-to-ND leg differences observed in jumping athletes. Jumping athletes exhibited D-to-ND leg differences in total proximal femur and femoral neck integral and cortical vBMD; however, the differences were not greater than D-to-ND leg differences observed in controls, except for integral vBMD at the femoral neck. The limited leg differences in jumping athletes relative to baseball pitchers may relate to the timing, duration and frequency of jumping exposure in the athletes tested. Jumping athletes began competing in jump events at the approximately the same time as their self-reported adolescent growth spurt and had been competing for approximately a third as long in their chosen sport compared to the baseball pitchers. The later introduction and shorter duration of unilateral loading may have tempered side-to-side differences in jumpers. We also hypothesize that the jumping athletes performed less frequent and fewer repetitions of unilateral loading compared to baseball pitchers who perform hundreds of weekly repetitions.

Jumping athletes also perform a high volume of bilateral loading activities, such as sprinting, which may enhance proximal femur bone health bilaterally. The latter was evident by jumpers having greater estimated strength in their ND leg compared to both pitchers and controls (Supplementary Table 2). The net result is enhancement of the denominator in calculations of side-to-side differences in jumpers and a subsequent reduction in D-to-ND leg percent differences. In contrast, the ND leg in pitchers is less frequently loaded beyond habitual levels making this population a better within-subject controlled model, with the proximal femur in the ND leg in pitchers in the current study having equivalent properties to the ND leg of controls (Supplementary Tables 1&2). In individuals who throw and hit on the same side of their body (e.g. all participants in the current study), the ND leg (right leg in right handed throwers and hitters) is exposed to habitual level loads (1× body weight).<sup>(40, 53–55)</sup> In contrast, the D leg is exposed to 25–50% and 75–100% higher loads during hitting and pitching, respectively.<sup>(40, 54–56)</sup>

Our study had a number of strengths, including the use of a within-subject controlled model to control selection bias and minimize the impact of inherited and systemic factors, and the inclusion of a control group not exposed to unilaterally elevated loads to account for any normal crossed asymmetry. However, the study also possesses limitations. We studied a limited number of subjects which may have reduced our ability to detect small D-to-ND leg differences. Small effects may be clinically relevant, particularly in those with compromised bone health. We did not quantify the pattern of proximal femur loading during pitching or jumping to correlate with the observed adaptation patterns, nor did we assess retrospective or current training volumes to explore unilateral loading dose effects. The current study focused on adaptation in males only. Females are at greater risk of proximal femur fracture and may not show the same adaptation pattern as males. We previously observed female fast-pitch softball pitchers exhibited larger D-to-ND leg differences than male baseball pitchers when assessed using DXA.<sup>(19)</sup> CT partial volume effects resulting from a tradeoff between spatial resolution and radiation dose may have influenced our ability to identify small changes, particularly at the relatively thin superior femoral neck. However, our cortical bone thickness quantification method takes into consideration partial volume effects.<sup>(22)</sup> Changes in bone thickness could have been smaller than the 3 mm finite elements used in our FE models. Any increase in thickness would be included in the calculation of an element's material properties, thereby influencing its mechanical properties; however, the relatively large size of the elements may have resulted in a loss of precision compromising our ability to identify D-to-ND leg differences. Finally, our FE models explored bone strength under only two representative load conditions. The possibility for different outcomes under alternative loading conditions cannot be excluded.

In summary, the current data demonstrate the heterogeneous adaptation of the proximal femur to chronic weight bearing-directed loading. Adaptation was principally observed in the inferior aspect of the femur neck and at the greater trochanter, and increased proximal femur strength under single-leg stance loading. In contrast, there was no to minimal adaptation at the superior femoral neck or benefit of the observed adaptation on femur ultimate strength to fracture-relevant loading due to a fall on the greater trochanter. These data raise questions as to how to better target physical activity toward the superior femoral neck and increase breaking strength to common injurious loading during aging (i.e. a fall onto the greater trochanter).

## Supplementary Material

Refer to Web version on PubMed Central for supplementary material.

## ACKNOWLEDGEMENTS

This contribution was made possible by support from the National Institutes of Health (P30 AR072581, R01 AR057740, R01 AR064140 and R01 AR068456).

## REFERENCES

1. Nikander R, Sievanen H, Heinonen A, Daly RM, Uusi-Rasi K, Kannus P. Targeted exercise against osteoporosis: a systematic review and meta-analysis for optimising bone strength throughout life. *BMC Med.* 2010;8:47. [PubMed: 20663158]

2. Tan VP, Macdonald HM, Kim S, et al. Influence of physical activity on bone strength in children and adolescents: a systematic review and narrative synthesis. *J Bone Miner Res.* 2014;29:2161–81. [PubMed: 24737388]
3. Xu J, Lombardi G, Jiao W, Banfi G. Effects of exercise on bone status in female subjects, from young girls to postmenopausal women: an overview of systematic reviews and meta-analyses. *Sports Med.* 2016;46:1165–82. [PubMed: 26856338]
4. Fuchs RK, Kersh ME, Carballido-Gamio J, Thompson WR, Keyak JH, Warden SJ. Physical activity for strengthening fracture prone regions of the proximal femur. *Curr Osteoporos Rep.* 2017;15:43–52. [PubMed: 28133707]
5. Parkkari J, Kannus P, Palvanen M, et al. Majority of hip fractures occur as a result of a fall and impact on the greater trochanter of the femur: a prospective controlled hip fracture study with 206 consecutive patients. *Calcif Tissue Int.* 1999;65:183–7. [PubMed: 10441647]
6. Nevitt MC, Cummings SR. Type of fall and risk of hip and wrist fractures: the study of osteoporotic fractures. The Study of Osteoporotic Fractures Research Group. *J Am Geriatr Soc.* 1993;41:1226–34. [PubMed: 8227898]
7. Cristofolini L. In vitro evidence of the structural optimization of the human skeletal bones. *J Biomech.* 2015;48:787–96. [PubMed: 25596628]
8. Kersh ME, Martelli S, Zebaze R, Seeman E, Pandy MG. Mechanical loading of the femoral neck in human locomotion. *J Bone Miner Res.* 2018;33:1999–2006. [PubMed: 29920773]
9. Lotz JC, Cheal EJ, Hayes WC. Stress distributions within the proximal femur during gait and falls: implications for osteoporotic fracture. *Osteoporos Int.* 1995;5:252–61. [PubMed: 7492864]
10. Zani L, Erani P, Grassi L, Taddei F, Cristofolini L. Strain distribution in the proximal human femur during in vitro simulated sideways fall. *J Biomech.* 2015;48:2130–43. [PubMed: 25843261]
11. Kersh ME, Pandy MG, Bui QM, et al. The heterogeneity in femoral neck structure and strength. *J Bone Miner Res.* 2013;28:1022–8. [PubMed: 23197364]
12. Verhulp E, van Rietbergen B, Huiskes R. Load distribution in the healthy and osteoporotic human proximal femur during a fall to the side. *Bone.* 2008;42:30–5. [PubMed: 17977813]
13. de Bakker PM, Manske SL, Ebacher V, Oxland TR, Crompton PA, Guy P. During sideways falls proximal femur fractures initiate in the superolateral cortex: evidence from high-speed video of simulated fractures. *J Biomech.* 2009;42:1917–25. [PubMed: 19524929]
14. Juszczuk MM, Cristofolini L, Salva M, Zani L, Schileo E, Viceconti M. Accurate in vitro identification of fracture onset in bones: failure mechanism of the proximal human femur. *J Biomech.* 2013;46:158–64. [PubMed: 23218142]
15. Abe S, Narra N, Nikander R, Hyttinen J, Kouhia R, Sievanen H. Exercise loading history and femoral neck strength in a sideways fall: a three-dimensional finite element modeling study. *Bone.* 2016;92:9–17. [PubMed: 27477004]
16. Allison SJ, Poole KE, Treece GM, et al. The influence of high-impact exercise on cortical and trabecular bone mineral content and 3D distribution across the proximal femur in older men: a randomized controlled unilateral intervention. *J Bone Miner Res.* 2015;30:1709–16. [PubMed: 25753495]
17. Lang TF, Saeed IH, Streeter T, et al. Spatial heterogeneity in the response of the proximal femur to two lower-body resistance exercise regimens. *J Bone Miner Res.* 2014;29:1337–45. [PubMed: 24293094]
18. Nikander R, Kannus P, Dastidar P, et al. Targeted exercises against hip fragility. *Osteoporos Int.* 2009;20:1321–8. [PubMed: 19002370]
19. Fuchs RK, Thompson WR, Weatherholt AM, Warden SJ. Baseball and softball pitchers are distinct within-subject controlled models for exploring proximal femur adaptation to physical activity. *Calcif Tissue Int.* 2019;104:373–81. [PubMed: 30666354]
20. Gümü tekin K, Akar S, Dane S, Yildirim M, Seven B, Varoglu E. Handedness and bilateral femoral bone densities in men and women. *Int J Neurosci.* 2004;114:1533–47. [PubMed: 15512837]
21. Lang T, LeBlanc A, Evans H, Lu Y, Genant H, Yu A. Cortical and trabecular bone mineral loss from the spine and hip in long-duration spaceflight. *J Bone Miner Res.* 2004;19:1006–12. [PubMed: 15125798]

22. Carballido-Gamio J, Bonaretti S, Saeed I, et al. Automatic multi-parametric quantification of the proximal femur with quantitative computed tomography. *Quant Imaging Med Surg.* 2015;5:552–68. [PubMed: 26435919]
23. Lang TF, Keyak JH, Heitz MW, et al. Volumetric quantitative computed tomography of the proximal femur: precision and relation to bone strength. *Bone.* 1997;21:101–8. [PubMed: 9213015]
24. Carballido-Gamio J, Harnish R, Saeed I, et al. Proximal femoral density distribution and structure in relation to age and hip fracture risk in women. *J Bone Miner Res.* 2013;28:537–46. [PubMed: 23109068]
25. Treece GM, Gee AH, Mayhew PM, Poole KE. High resolution cortical bone thickness measurement from clinical CT data. *Med Image Anal.* 2010;14:276–90. [PubMed: 20163980]
26. Yu A, Carballido-Gamio J, Wang L, et al. Spatial differences in the distribution of bone between femoral neck and trochanteric fractures. *J Bone Miner Res.* 2017;32:1672–80. [PubMed: 28407298]
27. Keyak JH. Improved prediction of proximal femoral fracture load using nonlinear finite element models. *Med Eng Phys.* 2001;23:165–73. [PubMed: 11410381]
28. Keyak JH, Kaneko TS, Tehranzadeh J, Skinner HB. Predicting proximal femoral strength using structural engineering models. *Clin Orthop Relat Res.* 2005:219–28.
29. Keyak JH, Koyama AK, LeBlanc A, Lu Y, Lang TF. Reduction in proximal femoral strength due to long-duration spaceflight. *Bone.* 2009;44:449–53. [PubMed: 19100348]
30. Keyak JH, Rossi SA, Jones KA, Skinner HB. Prediction of femoral fracture load using automated finite element modeling. *J Biomech.* 1998;31:125–33. [PubMed: 9593205]
31. Keyak JH, Sigurdsson S, Karlsdottir G, et al. Male-female differences in the association between incident hip fracture and proximal femoral strength: a finite element analysis study. *Bone.* 2011;48:1239–45. [PubMed: 21419886]
32. Keyak JH, Sigurdsson S, Karlsdottir GS, et al. Effect of finite element model loading condition on fracture risk assessment in men and women: the AGES-Reykjavik study. *Bone.* 2013;57:18–29. [PubMed: 23907032]
33. Gee AH, Treece GM. Systematic misregistration and the statistical analysis of surface data. *Med Image Anal.* 2014;18:385–93. [PubMed: 24440743]
34. Treece GM, Gee AH, Tonkin C, et al., Osteoporotic Fractures in Men Study. Predicting hip fracture type with cortical bone mapping (CBM) in the Osteoporotic Fractures in Men (MrOS) Study. *J Bone Miner Res.* 2015;30:2067–77. [PubMed: 25982802]
35. Genovese CR, Lazar NA, Nichols T. Thresholding of statistical maps in functional neuroimaging using the false discovery rate. *Neuroimage.* 2002;15:870–8. [PubMed: 11906227]
36. Keyak JH, Rossi SA, Jones KA, Les CM, Skinner HB. Prediction of fracture location in the proximal femur using finite element models. *Med Eng Phys.* 2001;23:657–64. [PubMed: 11755810]
37. Coh M, Supej M. Biomechanical model of the take-off action in the high jump: a case study. *New Stud Athlet.* 2008;23:63–73.
38. Kageyama M, Sugiyama T, Kanehisa H, Maeda A. Difference between adolescent and collegiate baseball pitchers in the kinematics and kinetics of the lower limbs and trunk during pitching motion. *J Sports Sci Med.* 2015;14:246–55. [PubMed: 25983571]
39. Luhtanen P, Komi PV. Mechanical power and segmental contribution to force impulses in long jump take-off. *Eur J Appl Physiol Occup Physiol.* 1979;41(4):267–74. [PubMed: 499190]
40. MacWilliams BA, Choi T, Perezous MK, Chao EY, McFarland EG. Characteristic ground-reaction forces in baseball pitching. *Am J Sports Med.* 1998;26:66–71. [PubMed: 9474404]
41. Mero A, Komi PV. Force-, EMG-, and elasticity-velocity relationships at submaximal, maximal and supramaximal running speeds in sprinters. *Eur J Appl Physiol Occup Physiol.* 1986;55:553–61. [PubMed: 3769912]
42. Werner SL, Guido JA, McNeice RP, Richardson JL, Delude NA, Stewart GW. Biomechanics of youth windmill softball pitching. *Am J Sports Med.* 2005;33:552–60. [PubMed: 15722291]
43. Poole KE, Mayhew PM, Rose CM, et al. Changing structure of the femoral neck across the adult female lifespan. *J Bone Miner Res.* 2010;25:482–91. [PubMed: 19594320]



44. Johannesdottir F, Poole KE, Reeve J, et al. Distribution of cortical bone in the femoral neck and hip fracture: a prospective case-control analysis of 143 incident hip fractures; the AGES-REYKJAVIK Study. *Bone*. 2011;48:1268–76. [PubMed: 21473947]
45. Poole KES, Skingle L, Gee AH, et al. Focal osteoporosis defects play a key role in hip fracture. *Bone*. 2017;94:124–34. [PubMed: 27777119]
46. Järvinen TLN, Kannus P, Sievänen H. Have the DXA-based exercise studies seriously underestimated the effects of mechanical loading on bone? *J Bone Miner Res*. 1999;14:1634–5. [PubMed: 10469294]
47. Warden SJ, Mantila Roosa SM, Kersh ME, et al. Physical activity when young provides lifelong benefits to cortical bone size and strength in men. *Proc Natl Acad Sci U S A*. 2014;111:5337–42. [PubMed: 24706816]
48. Michalski AS, Amin S, Cheung AM, et al. Hip load capacity cut-points for Astronaut Skeletal Health NASA Finite Element Strength Task Group Recommendations. *NPJ Microgravity*. 2019;5:6. [PubMed: 30886891]
49. Abe S, Narra N, Nikander R, Hyttinen J, Kouhia R, Sievanen H. Impact loading history modulates hip fracture load and location: A finite element simulation study of the proximal femur in female athletes. *J Biomech*. 2018;76:136–43. [PubMed: 29921524]
50. Poole KE, Treece GM, Gee AH, et al. Denosumab rapidly increases cortical bone in key locations of the femur: a 3D bone mapping study in women with osteoporosis. *J Bone Miner Res*. 2015;30:46–54. [PubMed: 25088963]
51. Deng C, Gillette JC, Derrick TR. Femoral neck stress in older adults during stair ascent and descent. *J Appl Biomech*. 2018;34:191–8. [PubMed: 29283748]
52. Martelli S, Kersh ME, Schache AG, Pandy MG. Strain energy in the femoral neck during exercise. *J Biomech*. 2014;47:1784–91. [PubMed: 24746018]
53. Elliott B, Grove JR, Gibson B. Timing of the lower limb drive and throwing limb movement in baseball pitching. *Int J Sports Biomech*. 1988;4:59–67.
54. Fortenbaugh D, Fleisig G, Onar-Thomas A, Asfour S. The effect of pitch type on ground reaction forces in the baseball swing. *Sports Biomech*. 2011;10:270–9. [PubMed: 22303780]
55. Welch CM, Banks SA, Cook FF, Draovitch P. Hitting a baseball: a biomechanical description. *J Orthop Sports Phys Ther*. 1995;22:193–201. [PubMed: 8580946]
56. Guido JA Jr, Werner SL. Lower-extremity ground reaction forces in collegiate baseball pitchers. *J Strength Cond Res*. 2012;26:1782–5. [PubMed: 22344047]

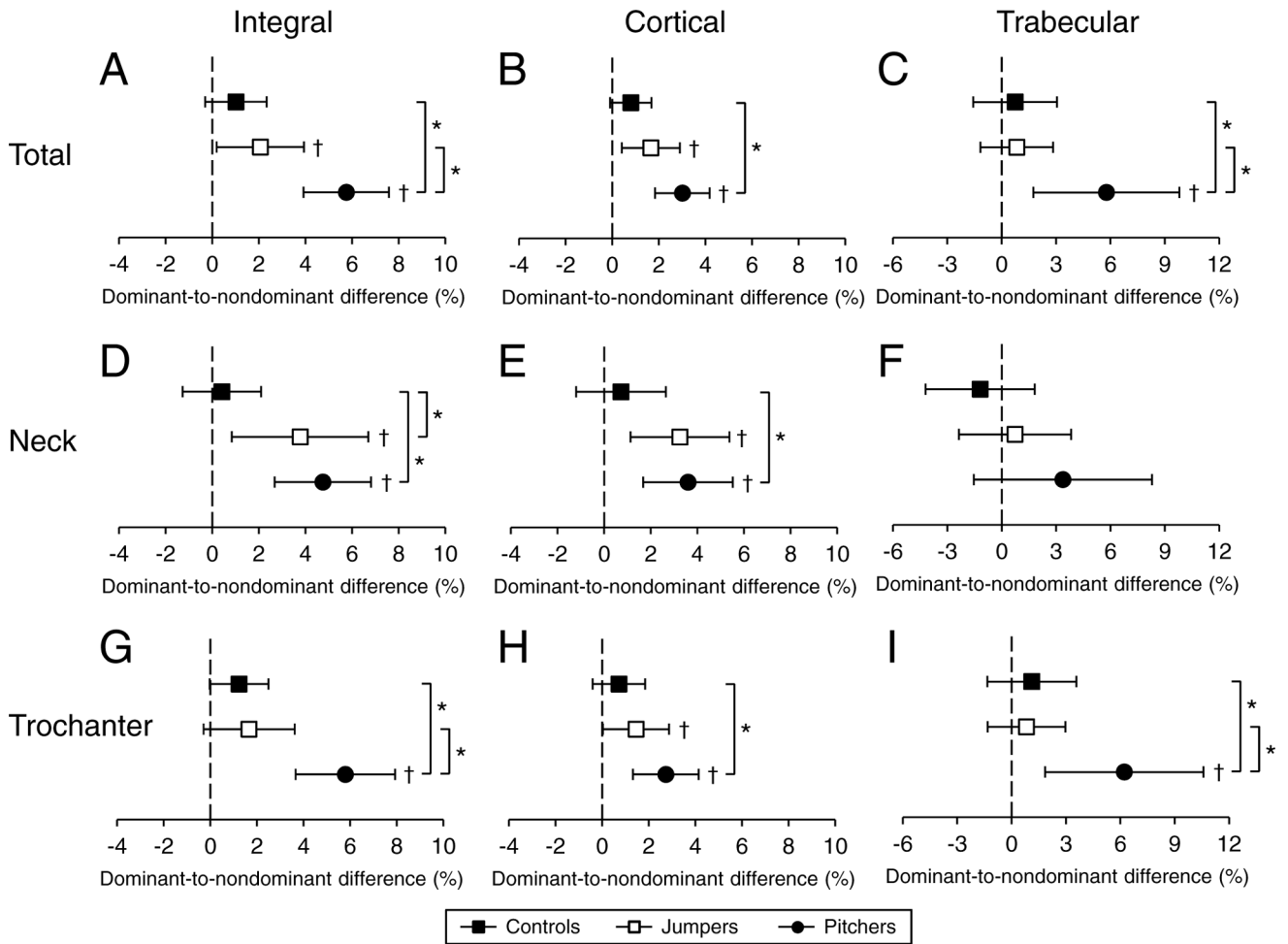


**Figure 1.** Percent dominant-to-nondominant leg differences for integral (i.e. cortical + trabecular), cortical and trabecular vBMD in the total proximal femur (A-C), femoral neck (D-F), and trochanter (G-I) regions. Data represent mean percent difference between the dominant and nondominant legs, with error bars indicating 95% confidence intervals. Confidence intervals greater than 0% (†) indicate greater bone properties within the dominant leg compared to nondominant leg. \*indicates  $p < 0.05$  for between group comparison.

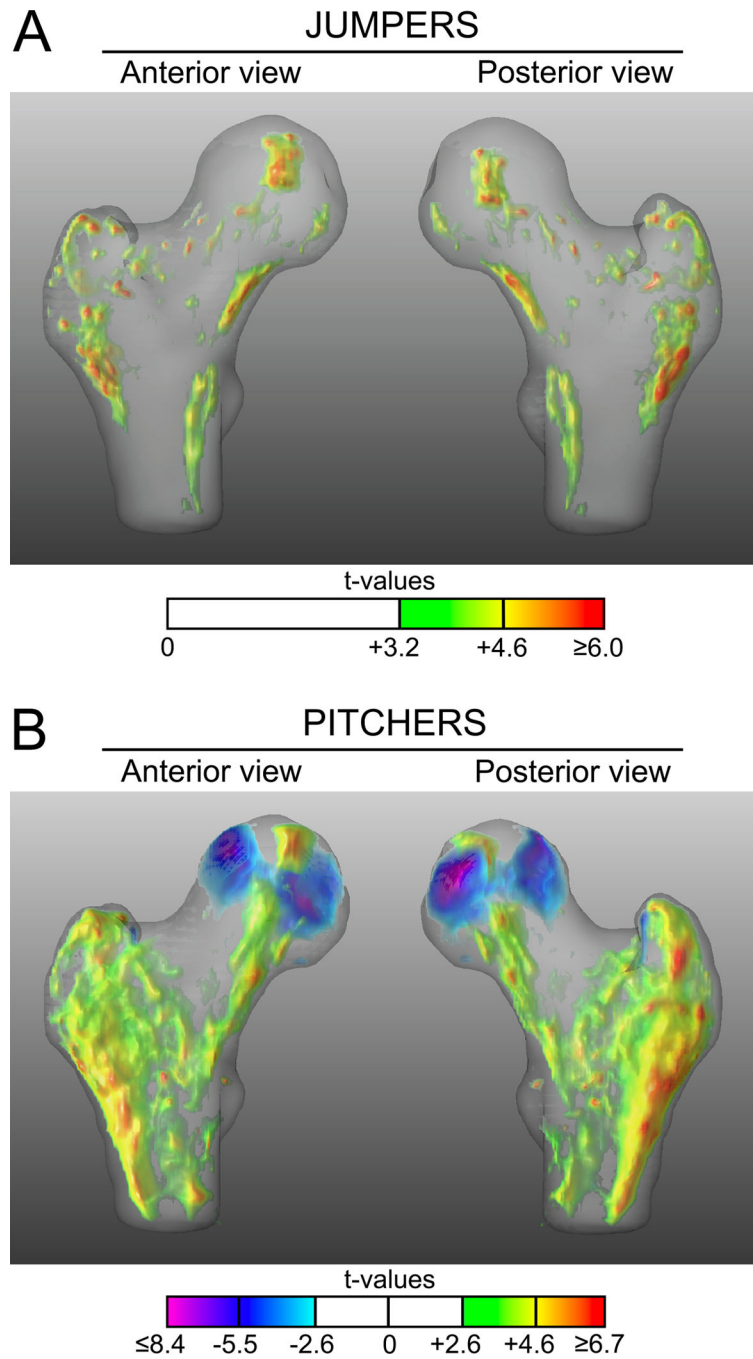


**Figure 2.** Anterior and posterior views of the 3D t-map showing voxel-wise differences in vBMD between the dominant and nondominant legs in jumpers (A) and pitchers (B). Voxels with positive and negative t-values indicate significantly higher and lower vBMD in dominant legs compared to contralateral nondominant legs, respectively. Voxels where there were no statistical differences between dominant and nondominant legs are rendered transparent.

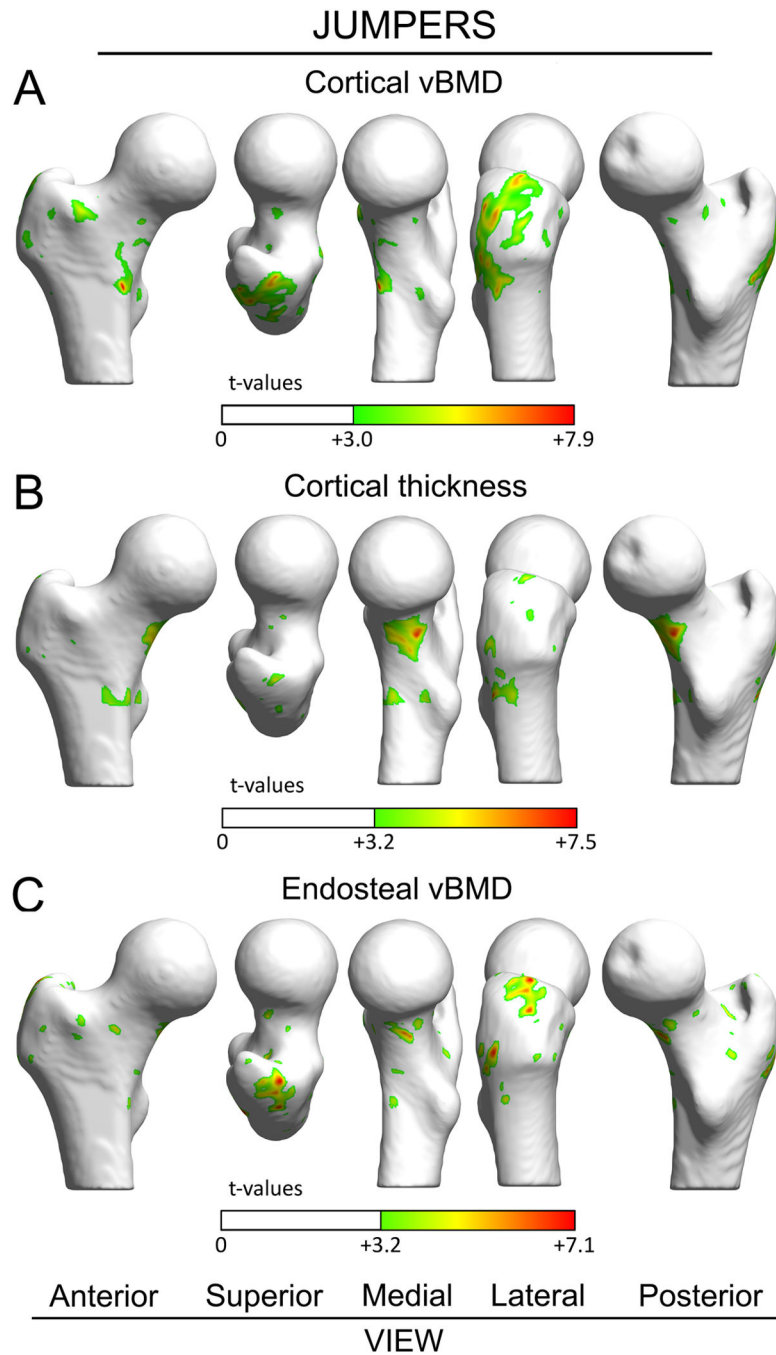


**Figure 3.** Surface-based maps of vertex-wise differences between dominant and nondominant legs in jumpers for cortical vBMD (A), Ct.Th (B), and EndoTb.vBMD (C). Vertices with positive t-values indicate significantly greater properties within dominant legs compared to contralateral nondominant legs. Vertices where there were no differences between dominant and nondominant legs are rendered white. The femoral head was excluded from the analyses due to its thin cortical bone.

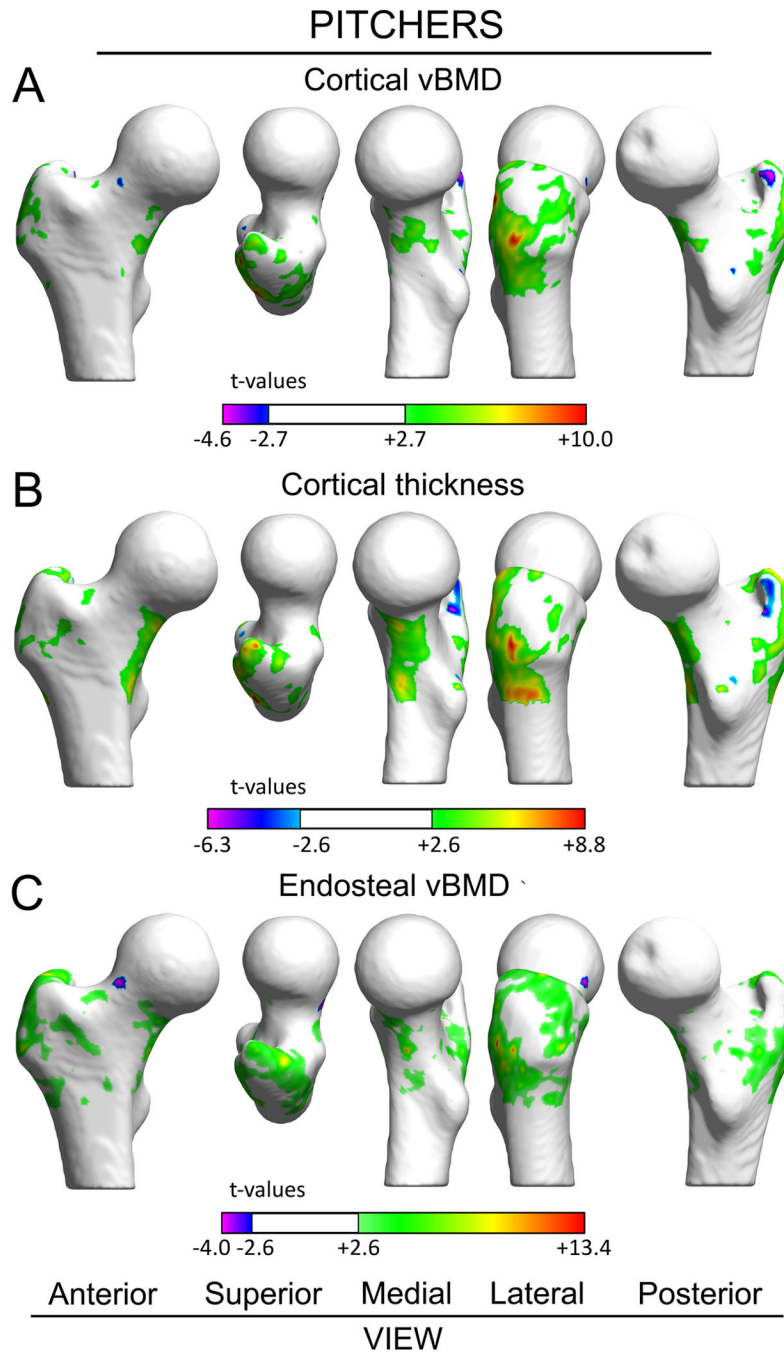


**Figure 4.** Surface-based maps of vertex-wise differences between dominant and nondominant legs in pitchers for cortical vBMD (A), Ct.Th (B), and EndoTb.vBMD (C). Vertices with positive and negative t-values indicate significantly greater and lesser properties within dominant legs compared to contralateral nondominant legs, respectively. Vertices where there were no differences between dominant and nondominant legs are rendered white. The femoral head was excluded from the analyses due to its thin cortical bone.

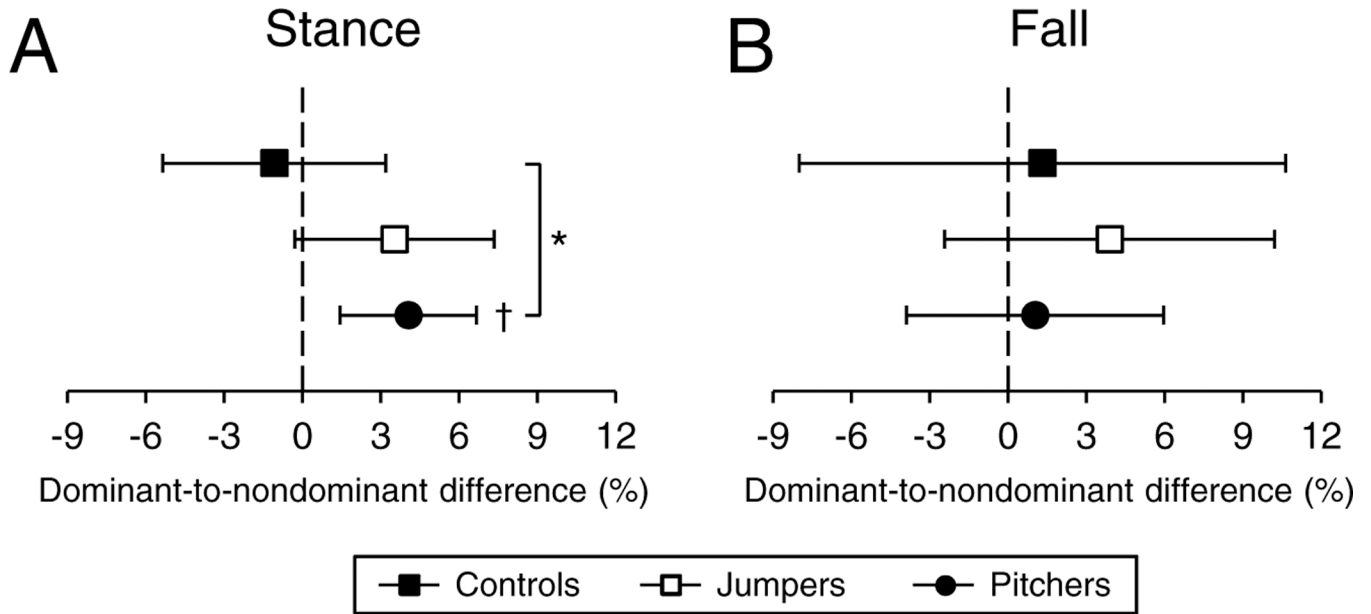


**Figure 5.**

Percent dominant-to-nondominant leg differences for proximal femur ultimate strength under single-leg stance loading (A), and yield (B) and ultimate (C) strength under loading associated with a fall onto the posterolateral greater trochanter. Data represent mean percent difference between the dominant and nondominant legs, with error bars indicating 95% confidence intervals. Confidence intervals greater than 0% (†) indicate greater bone strength within the dominant leg compared to nondominant leg. \*indicates  $p < 0.05$  for between group comparison.



**Table 1.** Demographic and anthropometric characteristics of controls, jumpers and pitchers<sup>‡</sup>

Characteristic	Controls	Jumpers	Pitchers
<i>n</i>	15	16	16
<i>Demographics</i>			
Age (yr)	22.1 ± 2.7 <sup>P</sup>	21.1 ± 2.1 <sup>P</sup>	26.8 ± 2.1 <sup>CJ</sup>
Dominant leg (R/L)	0/15	4/12	3/13
Estimated age of adolescent growth spurt (yr)	13.9 ± 1.9	13.8 ± 1.8	14.2 ± 1.4
Age started competing (yr)	–	13.6 ± 1.5 <sup>P</sup>	8.5 ± 2.5 <sup>J</sup>
Years competing before adolescent growth spurt (yr)	–	0.3 ± 2.1 <sup>P</sup>	5.6 ± 1.9 <sup>J</sup>
Total years competing (yr)	–	6.3 ± 2.7 <sup>P</sup>	18.1 ± 2.9 <sup>J</sup>
Jumping sport (long:high jump)	–	12:10 <sup>‡</sup>	–
Jump training per week (min)	–	213 ± 126	–
Jumps per week (n)	–	72 ± 55	–
Personal best: long jump (m)	–	7.18 ± 0.57	–
Personal best: high jump (m)	–	2.06 ± 0.12	–
Professional baseball games played (n)	–	–	181 ± 89
Professional baseball innings pitched (n)	–	–	616 ± 334
<i>Whole-body anthropometry</i>			
Height (m)	1.79 ± 0.07 <sup>P</sup>	1.83 ± 0.07 <sup>P</sup>	1.92 ± 0.05 <sup>CJ</sup>
Mass (kg)	67.7 ± 7.4 <sup>P</sup>	78.3 ± 6.9 <sup>CP</sup>	94.4 ± 8.5 <sup>CJ</sup>
Body mass index (kg/m <sup>2</sup> )	21.1 ± 1.7 <sup>P</sup>	23.5 ± 1.9 <sup>CP</sup>	25.5 ± 2.0 <sup>CJ</sup>
Areal bone mineral density (g/cm <sup>2</sup> ) <sup>#</sup>	1.19 ± 0.09 <sup>P</sup>	1.38 ± 0.9 <sup>C</sup>	1.32 ± 0.15 <sup>C</sup>
Lean mass (kg) <sup>§</sup>	52.3 ± 5.1 <sup>P</sup>	59.2 ± 5.1 <sup>C</sup>	63.5 ± 5.5 <sup>C</sup>
Fat mass (%)	16.2 ± 4.0 <sup>P</sup>	14.0 ± 2.0 <sup>P</sup>	21.2 ± 3.2 <sup>CJ</sup>

<sup>‡</sup>Data are mean ± SD, except for frequencies. Superscript capital letters indicate the data significantly differs from controls (C), jumpers (J) and pitchers (P)

<sup>§</sup>Six jumpers competed in both jumping sports

<sup>#</sup>Values corrected for age and whole-body lean mass

<sup>§</sup>Values corrected for age and height